Inorg. Chem. **2002**, *41*, 5203–5215

Charge-Transfer Spectra of Structurally Characterized Mixed-Valence Thiolate-Bridged Cu(I)/Cu(II) Cluster Complexes

Robert T. Stibrany, Ronald Fikar, Mark Brader, Marc N. Potenza, Joseph A. Potenza,* and Harvey J. Schugar*

Department of Chemistry and Chemical Biology, Rutgers, The State University of New Jersey, 610 Taylor Road, Piscataway, New Jersey 08854

Received February 25, 2002

A series of Cu(II) and Cu(I)/Cu(II) complexes containing the *cis*-N(amine)$_2$S(thiolate)$_2$ copper complex ***rac*-2** has been synthesized to provide a basis for understanding the charge-transfer spectra of mixed-valence thiolate-bridged Cu(I)/Cu(II) complexes. In combination with Cu(Me$_2$-13-N$_4$ane), ***rac*-2** yields a monobridged dinuclear homovalent adduct, ***rac*-5**, while reaction with CuCl yields the mixed-valance pentanuclear complex ***rac*-6**. In the presence of Cu(II)(acac)$_2$, chiral ***R,R*-1** reacts to form a mixed-valence pentanuclear cation ***R,R*-7**. ***rac*-6** exhibits a relatively short Cu(I)···Cu(II) contact [2.8231(9) Å] and associated structural features that suggest the presence of a weak Cu(I)···Cu(II) interaction in a valence-trapped system. Additional structural features in ***rac*-6** and ***R,R*-7** include singly and doubly bridging thiolates, three- and four-coordinated Cu(I) ions, and varying Cu(I) ligand sets. These features extend the types and complexities of electronic absorptions significantly. Spectra of ***rac*-6** and ***R,R*-7** exhibit multiple overlapping absorptions over the entire visible and ultraviolet spectral regions studied, consonant with these observations. Trends resulting from variations in structure type and oxidation state permit a first approach toward developing a detailed assignment of the individual ligand Rydberg, LF, LMCT, MLCT, and possible MMCT absorptions in these complexes.

Introduction

Our long-term interest in copper and sulfur chemistry has led us to prepare various stable thioether,[1] thiolate,[2] persulfide,[3] disulfide,[4] and cluster complexes[5] of Cu(II) and/or Cu(I). We now present a first approach toward developing a detailed assignment of the individual ligand Rydberg, LF, LMCT, MLCT, and possible MMCT absorptions in mixed-valence polynuclear Cu(I)/Cu(II) cluster complexes containing bridging thiolate ligands. Dinuclear thiolate-bridged Cu(II) complexes[6] have been characterized structurally, as have dinuclear, trinuclear,[7] and pentanuclear[5a,8] mixed-valence Cu(I)/Cu(II) species, but a detailed interpretation of the rich electronic spectra shown by these highly colored species is lacking. Electronic spectra of dinuclear mixed-valence thiolate-bridged Cu(I)/Cu(II) systems are of biological importance owing to their presence in Cu$_A$-type electron-transfer sites in proteins.[9] Higher order clusters present the challenge of identifying how incorporation of Cu(II) subunits perturbs the electronic spectra of the widely known thiolate-bridged Cu(I) clusters and how the spectra of mononuclear

* To whom correspondence should be addressed. E-mail: potenza@rutchem.rutgers.edu (J.A.P.).

(1) (a) Knpp, S.; Keenan, T. P.; Liu, J.; Potenza, J. A.; Schugar, H. J. *Inorg. Chem.* **1990**, *29*, 2189−2191. (b) Cohen, B.; Ou, C. C.; Lalancette, R. A.; Borowski, W.; Potenza, J. A.; Schugar, H. J. *Inorg. Chem.* **1979**, *18*, 217−220. (c) Ou, C. C.; Miskowski, V. M.; Lalancette, R. A.; Potenza, J. A.; Schugar, H. J. *Inorg. Chem.* **1976**, *15*, 3157−3161.

(2) (a) Bharadwaj, P.; Potenza, J. A.; Schugar, H. J. *J. Am. Chem. Soc.* **1986**, *108*, 1351−1352. (b) John, E.; Bharadwaj, P. K.; Potenza, J. A.; Schugar, H. J. *Inorg. Chem.* **1986**, *25*, 3065−3069. (c) Hughey, J. L., IV; Fawcett, T. G.; Rudich, S. M.; Lalancette, R. A.; Potenza, J. A.; Schugar, H. J. *J. Am. Chem. Soc.* **1979**, *101*, 2617−2623.

(3) John, E.; Bharadwaj, P. K.; Krogh-Jespersen, K.; Potenza, J. A.; Schugar, H. J. *J. Am. Chem. Soc.* **1986**, *108*, 5015−5017.

(4) (a) Fox, S.; Stibrany, R. T.; Potenza, J. A.; Knapp, S.; Schugar, H. J. *Inorg. Chem.* **2000**, *39*, 4950−4961. (b) Fox, S.; Potenza, J. A.; Knapp, S.; Schugar, H. J. Copper(II) Complexes of Binucleating Macrocyclic Bis(disulfide) Tetramine Ligands. In *Bioinorganic Chemistry of Copper*; Karlin, K. D., Tyeklár, Z., Eds.; Chapman and Hall: New York, 1993; pp 35−47. (c) Thich, J. A.; Mastropaolo, D.; Potenza, J. A.; Schugar, H. J. *J. Am. Chem. Soc.* **1974**, *96*, 726−731.

(5) (a) Bharadwaj, P. K.; John, E.; Xie, C.-L.; Zhang, D.; Hendrickson, D. N.; Potenza, J. A.; Schugar, H. J. *Inorg. Chem.* **1986**, *25*, 4541−4546. (b) Schugar, H. J.; Ou, C.-C.; Thich, J. A.; Potenza, J. A.; Felthouse, T. R.; Hendrickson, D. N.; Furey, W., Jr.; Lalancette, R. A. *Inorg. Chem.* **1980**, *19*, 543−552.

(6) (a) Aoi, N.; Matsubayashi, G−e.; Tanaka, T. *J. Chem. Soc., Dalton Trans.* **1987**, 241−247. (b) Aoi, N.; Takano, Y.; Ogino, H.; Matsubayashi, G−e.; Tanaka, T. *J. Chem. Soc., Chem. Commun.* **1985**, 703−704.

(7) Houser, R. P.; Tolman, W. B. *Inorg. Chem.* **1995**, *34*, 1632−1633.

(8) Sukal, S.; Bradshaw, J. E.; He, J.; Yap, G. P. A.; Rheingold, A. L.; Kung, H. F.; Francesconi, L. C. *Polyhedron* **1999**, *18*, 7−17.

10.1021/ic020156v CCC: $22.00
Published on Web 09/07/2002

Cu(II)-thiolate units are perturbed by their incorporation into thiolate-bridged Cu(I) clusters.

Our strategy is first to synthesize reference mononuclear Cu(II) complexes and then to use them as building blocks to form mixed-valence polynuclear Cu(I)/Cu(II) adducts. Synthetic approaches to mononuclear complexes must circumvent the redox instability commonly exhibited by Cu(II)-thiolate complexes and overcome unfavorable ligand-field stabilization energies.[10] Redox-stable Cu(II)-thiolate complexes have been reviewed recently.[11] A flattened Cu(II)N_2-SS* mimic of "type 1.5" blue copper sites[12] is a notable recent addition to the Cu(II)-thiolate literature.[11]

Previously, we prepared the reference chiral *cis*-CuN_2S_2 complex **8**,[2a] whose stability is not derived from steric or electronic roles of the unligated methyl ester groups. We have now prepared even more stable *cis*-CuN_2S_2 analogues from ester-free, linear tetradentate amino thiolate ligands such as ***rac*-1**.

We report here the synthesis, characterization, and electronic spectra of four copper complexes with ***rac*-1**: a discrete Cu(II) monomer, a homovalent Cu(II) thiolate-bridged binculear complex, and two mixed-valence pentanuclear Cu(I)/Cu(II) complexes. Using this series, comparisons are drawn between the reference monomer spectra and deconvoluted spectra of their polynuclear Cu(I)/Cu(II) adducts. Variations in structure type and oxidation state permit detailed interpretation of the UV−vis/CD spectra. Selected EPR and magnetochemical data are also presented.

Experimental Section

General Procedures. Reagents were used as received or purified by standard methods.[13] Melting points were determined with a hot-stage apparatus and are uncorrected. Infrared spectra were measured using a Mattson Galaxy Series 5000 spectrophotometer. Densities of the crystalline products were measured by flotation.

1. Preparation of the Complexes. ***rac*-1** and its Cu(II) complex ***rac*-2** were prepared as described previously.[4a] Preparation of the dinuclear complex ***rac*-5·2ClO_4** and the pentanuclear complexes ***rac*-6** and ***R,R*-7·**Cl is outlined in Scheme 1.

rac*-5·2ClO_4.** Ligand 1,4,7,10-tetraaza-12,12-dimethylcyclotridecane (Me_2-13-N_4ane), **3**, was prepared by following a literature procedure.[14] Complex **4·**2ClO_4 was prepared in quantitative yield by evaporating in air an ethanol solution 0.2 M in both $Cu(ClO_4)_2$·$6H_2O$ and **3**. Attempts to prepare ***rac*-2** by ligand exchange of **4** with 2H-rac*-1** resulted in the dinuclear adduct ***rac*-5**. A solution of **4·**2ClO_4 (0.06 g, 0.128 mmol) in a mixture of 5 g of DMF and 2 g of methanol was added to a mixture of crude 2H-***rac*-1** (0.09 g, 0.31 mmol) dissolved in 5 g of DMF and 5 g of ether. The resulting red solution was filtered (fine frit), deoxygenated by Ar bubbling, and left to stand in a sealed container at −10 °C for 2 weeks. A dark-red crystalline product was collected by filtration and dried in air. X-ray analysis showed the product (0.070 g, 0.085 mmol, 66% yield based upon **4**) to be the dinuclear adduct ***rac*-5·**2ClO_4, mp 109 °C (morphology change), 231 °C (sharp, decomp). IR (KBr pellet, cm^{-1}): 3276 m, 3113 w, 2943 m, 2859 m, 1653 w, 1457 m, 1091 s, 623 m. Anal. Calcd: N, 10.14; H, 6.57; C, 36.23; Cu, 15.33; Cl, 8.55. Found: N, 10.16; H, 6.72; C, 36.49; Cu, 15.43; Cl, 8.52.

***rac*-6·2DMF.** (a) This complex was first isolated from the reaction of ***rac*-2** with Cu(II)Cl_2·$2H_2O$. ***rac*-2** (0.05 g, 0.142 mmol) and Cu(II)Cl_2·$2H_2O$ (0.024 g, 0.142 mmol) were dissolved in 3 mL of DMF, filtered, deoxygenated by Ar bubbling, and placed in a freezer at −10 °C for 3 days. The green solution deposited a black crystalline solid, which was collected by filtration and dried in air (0.025 g, 0.022 mmol, 31% yield based on ***rac*-2**).

(b) ***rac*-6·**2DMF was later prepared directly by reacting ***rac*-2** with Cu(I)Cl. In a glovebox containing Ar, ***rac*-2** (0.050 g, 0.142 mmol) and Cu(I)Cl (0.021 g, 0.21 mmol) were dissolved in 5 mL of anhydrous DMF to give a very dark solution. After standing overnight, the solution deposited black crystalline blocks, which were collected by filtration and dried under Ar (0.052 g, 0.045 mmol, 64% yield based on ***rac*-2**). IR (KBr pellet, cm^{-1}): 3213 m, 2936 m, 2859 m, 1661 s, 1456 m, 1387 m, 1094 m.

(c) An attempt to prepare an analogue of ***rac*-6** with Cu(II) replaced by Zn(II) [e.g., Zn(***rac*-1**)$_2$·3CuCl] yielded ***rac*-6·**2DMF instead. In a glovebox containing Ar, Zn(II)(***rac*-1**)[21] (100 mg, 0.29 mmol) was dissolved in 15 mL of dry DMF to give a colorless solution. Then, Cu(I)Cl (80 mg, 0.81 mmol) was added. After stirring for 10 min the solution had darkened and was left undisturbed under Ar overnight, during which time dark-brown blocks precipitated. IR (KBr pellet, cm^{-1}): 3213 m, 2936 m, 2859 m, 1661 s, 1456 m, 1387 m, 1094 m. Anal. Calcd: N, 7.32; H, 6.15; C, 35.59; Cu, 27.69; Cl 9.27. Found: N, 7.22; H, 6.12; C, 35.49; Cu, 27.60; Cl, 9.42. X-ray fluorescence revealed no Zn above the detection limit (approximately 10 ppm).

X-ray crystal structures were obtained from all three preparations of ***rac*-6·**2DMF. The structure from preparation c is reported below.

R,R*-7Cl.** All manipulations were carried out under Ar using deoxygenated solvents. Resolved *trans*-cyclohexane diamine was obtained by following a literature procedure.[15] The appropriate enantiomer was used to prepare 2H-R,R*-1·**2HCl by following the procedure used for 2H-***rac*-1**.[4a] A solution containing 2H-***R,R*-1·**2HCl (250 mg, 0.70 mmol) in 10 mL of acetonitrile turned dark red upon addition of Cu(acac)$_2$ (200 mg, 0.77 mmol). The solution was warmed and stirred for 30 min, then layered with 10 mL of

(9) Gamelin, D. R.; Randall, D. W.; Hay, M. T.; Houser, R. P.; Mulder, T. C.; Canters, G. W.; de Vries, S.; Tolman, W. B.; Lu, Y.; Solomon, E. I. *J. Am. Chem. Soc.* **1998**, *120*, 5246−5263.

(10) Solomon, E. I.; Hare, J. W.; Dooley, D. M.; Dawson, J. H.; Stephens, P. J.; Gray, H. B. *J. Am. Chem. Soc.* **1980**, *102*, 168−178.

(11) Mandal, S.; Das, G.; Singh, R.; Shukla, R.; Bharadwaj, P. K. *Coord. Chem. Rev.* **1997**, 191−235.

(12) (a) Holland, P. L.; Tolman, W. B. *J. Am. Chem. Soc.* **2000**, *122*, 6331−6332. (b) Brader, M. L.; Dunn, M. F. *J. Am. Chem. Soc.* **1990**, *112*, 4585−4587.

(13) Perrin, D. D.; Armarego, W. L. F.*Purification of Laboratory Chemicals*; Pergamon Press: New York, 1988.

(14) (a) Curtis, N. F.; Reader, G. W. *J. Chem Soc., Dalton Trans.* **1972**, 1453−1460. (b) Curtis, N. F.; Reader, G. W. *J. Chem. Soc. (A)* **1971**, 1771−1777.

(15) Gullotti, M.; Pasini, A.; Fantucci, P.; Ugo, R.; Gillard, R. D. *Gazz. Chim. Ital.* **1972**, *102*, 855−892.

(16) (a) Gagne, R. R.; Koval, C. A.; Lisensky, G. C. *Inorg. Chem.* **1980**, *19*, 2854−2855. (b) Gritzner, G.; Kuta, J. *Pure Appl. Chem.* **1984**, *56*, 461−466.

(17) (a). *Enraf-Nonius Structure Determination Package*; Enraf-Nonius: Delft, Holland, 1985. (b) Sheldrick, G. M. SHELXS-97. *Acta Crystallogr.* **1990**, *A46*, 467−73. (c) Sheldrick, G. M. *SHELXL-97*: *A Computer Program for the Refinement of Crystal Structures*; University of Göttingen: Germany. (d) Blessing, R. H. *Acta Crystallogr.* **1995**, *A51*, 33−38.

(18) Farrugia, L. J. *ORTEP3 for Windows*, version 1.0.5; University of Glasgow: Scotland, 1997.

(19) Hanss, J.; Krüger, H.-J. *Angew. Chem., Int. Ed. Engl.* **1996**, *35*, 2827−2830.

(20) Anderson, O. P.; Becher, J.; Frydendahl, H.; Taylor, L. F.; Toftlund, H. *J. Chem. Soc., Chem. Commun.* **1986**, 699−701.

(21) Potenza, M. N.; Stibrany, R. T.; Potenza, J. A.; Schugar, H. J. *Acta Crystallogr.* **1992**, *C48*, 454−457.

Scheme 1. Synthesis of the Diaminocyclohexane-Based Complexes

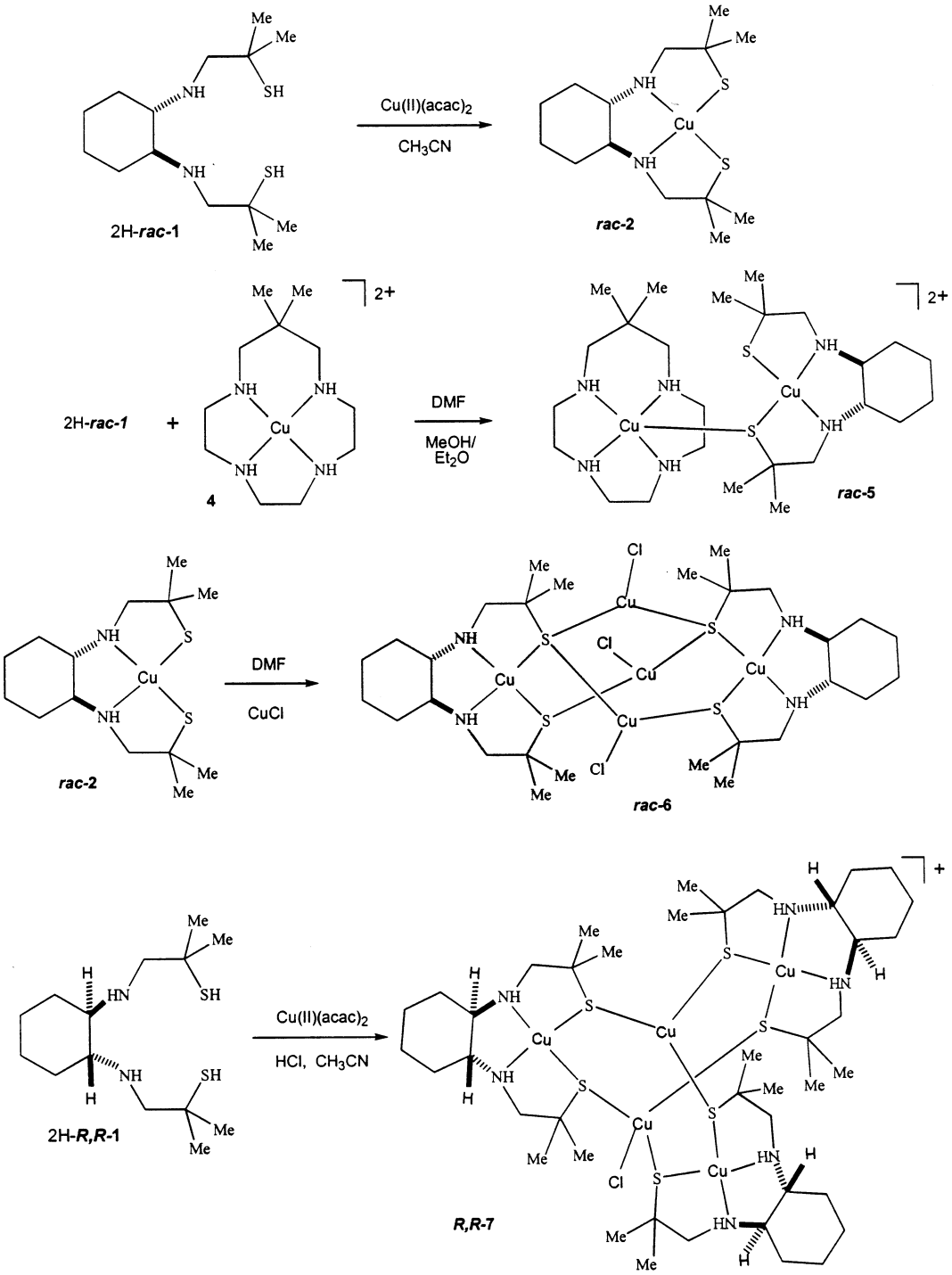

diethyl ether. Upon standing overnight, a black precipitate formed, which was recrystallized from 10 mL of 1:1 ethanol/diethyl ether in a freezer to yield chunky black prisms of solvated ***R,R*-7Cl**, some of which were vacuum-dried for elemental analysis**.** Anal. Calcd for [(***R,R*-2**)$_3$·Cu(I)Cl·Cu(I)]·Cl (vacuum-dried): N, 7.57; H, 6.77; C, 40.80; Cu, 24.53; Cl, 5.48. Found: N, 7.66; H, 6.72; C, 40.69; Cu, 24.43; Cl, 5.52.

2. Spectroscopic and Electrochemical Studies. Conventional and CD electronic spectral measurements were made using Cary instruments upgraded and computer-interfaced by Aviv Associates. Low-temperature (80 K) spectra were measured using an Air Products optical Dewar. EPR spectra were measured with a Varian E-12 spectrometer calibrated with a Hewlett-Packard Model 5245-L frequency counter and a DPPH crystal (g = 2.0036). ^{13}C and ^{1}H NMR spectra were recorded at room temperature using Varian XL-400 and Bruker AVANCE 400 Ultrashield spectrometers.

The magnetic susceptibility of ***rac*-2** was measured at 298(1) K using the Faraday technique; that of ***rac*-5** was determined from 10 to 300 K using a Quantum Design SQUID magnetometer operated at 1000 G. Diamagnetic corrections, calculated from Pascal's constants, were applied to the susceptibilities.

A Princeton Applied Research Model 173 potentiostat/galvanostat coupled with a model 175 current Follower and a model 175 Universal Programmer was used for cyclic voltammetry measure-

Table 1. Crystallographic Data for the Several Complexes Studied

	rac-**2**	***rac*-5**·2ClO_4	***rac*-6**·2DMF	***R,R*-7Cl**·solvate[a]
formula	$CuS_2N_2C_{14}H_{28}$	$Cu_2Cl_2S_2O_8N_6C_{25}H_{54}$	$Cu_5Cl_3S_4O_2N_6C_{34}H_{70}$	$Cu_5Cl_2S_6O_4N_{6.5}C_{52}H_{84}$
fw	352.06	828.84	1147.25	1445.22
a, Å	10.162(2)	15.147(3)	11.9583(15)	19.312(2)
b, Å	16.221(3)	15.324(3)	20.162(3)	19.312(2)
c, Å	10.332(1)	16.858(3)	21.430(3)	19.312(2)
β, deg	94.24(1)	106.492(3)	99.898(2)	90
V, Å^3	1698.4(5)	3752.1(12)	5089.8(11)	7202.5(13)
space group	$P2_1/c$	$P2_1/c$	$C2/c$	$P2_13$
Z	4	4	4	4
ρ_{calcd}, g/cm^3	1.377	1.467	1.497	1.33
r_{obsd}, g/cm^3	1.37(1)	1.45(1)	1.46(1)	1.36(1)
μ, mm^{-1}	1.52	1.44	2.41	1.74
transmn factor	0.96−1.00	0.77−1.00	0.68−1.00	0.89−1.00
T, K	297(1)	294(2)	295(1)	293(2)
no. of data used in refinement	2983	5355	3660	1255
R_F,[b] $R_{wF}{}^2$ [c]	0.029, 0.077	0.042, 0.106	0.038, 0.074	0.040, 0.099

[a] See text for formula of solvate. [b] $R_F = \sum||F_o| - |F_c||/\sum|F_o|$; selection criterion $I > 2\sigma(I)$. [c] $R_{wF}{}^2 = \{[\sum[w(F_o{}^2 - F_c{}^2)^2/\sum[w(F_o{}^2)^2]\}^{1/2}$; selection criterion all $F_o{}^2$.

ments which were performed at 23(1) °C on a 5 mM solution of ***rac*-2** in acetonitrile containing 0.1 M tetraethylammonium tetrafluoroborate. A PAR cell with a three-electrode configuration (platinum button working electrode, Ag/Ag^+ (0.1 M $AgNO_3$ in CH_3CN) pseudo-reference electrode, and a Pt wire auxiliary electrode) was used. Ferrocene/ferrocenium was used as an internal standard for referencing potentials to the NHE.[16] No corrections were made for liquid junction potentials. Solutions were deoxygenated by bubbling Ar through them, and voltammograms were recorded with the solutions under an Ar atmosphere.

3. Crystallography. For ***rac*-2** and ***R,R*-7**, diffraction measurements were made on an Enraf-Nonius CAD-4 diffractometer, and the Nonius Structure Determination Package[17a] was used for data collection and processing. Data for ***rac*-5** and ***rac*-6** were collected using a Bruker SMART CCD area detector system, and absorption corrections were applied using program SADABS.[17d] In all cases, graphite monochromated Mo Kα radiation was used, and Lorentz, polarization, decay, and absorption corrections were applied.

Structures were solved and refined on F^2 using the SHELX system and all data.[17b,c] Partial structures were obtained by direct methods; the remaining non-hydrogen atoms were located using difference Fourier techniques. H atoms were located on difference maps or placed at calculated positions and refined when possible. Views of the structures were prepared using ORTEP3 for Windows.[18]

Crystals of ***rac*-2, *rac*-5**·2ClO_4, and ***rac*-6**·2DMF were mounted on glass rods. The structures refined smoothly except for one perchlorate group in ***rac*-5**·2ClO_4, which exhibited a two-site positional disorder. For ***R,R*-7Cl**·solvate, a crystal was mounted in a sealed capillary tube along with some mother liquor. The ***R,R*-7** cations were located easily and refined smoothly; however, the chloride anion and solvate regions exhibited disorder. The best model that accounted for all electron density with no unusual intermolecular contacts gave the empirical formula ***R,R*-7Cl**·$(CH_3CH_2)_2O$·2.5CH_3CH_2OH·0.5CH_3CN·0.5H_2O. Additional crystallographic details are given in Table 1 and as Supporting Information.

Results and Discussion

Description of the Structures. The structure of ***rac*-2** (Figure 1) consists of discrete molecules with each copper ion exhibiting distorted square-planar N_2(amine)S_2(thiolate) coordination (Table 2). Many of the structural details of ***rac*-2** compare well with those reported for related structures such as **8**−**12**[2a,7,19,20] (Chart 1, Table 3) and ***rac*-5** (Table 2), each of which contains one *cis*-Cu(II)N_2S(thiolate)$_2$ unit. In this group, the Cu(II)−N distances span a larger range (1.962(2)−2.059(13) Å) than the Cu(II)−S distances (2.2228(11)−2.262(4) Å), consistent with a greater variation in the structural type of the ligating nitrogen atoms. In these systems, the tetrahedral distortion dihedral angles S(1)−Cu−S(2)/N(1)−Cu−N(2) range from essentially zero in **9** to 51.9° in **12**, which contains a pair of NS ligands distorted toward tetrahedral by the diphenyl scaffolding. As expected, the zinc analogue of ***rac*-2**, Zn(II)(***rac*-1**), has a more nearly tetrahedral coordination geometry [S−Zn−S/N−Zn−N dihedral angle (70.99(5)°] and a correspondingly long S(1)···S(2) distance (4.240(1) Å).[21]

***rac*-2** forms an integral part of the ***rac*-5** and ***rac*-6** structures. In ***rac*-5**, S2 is bridging and acts as a fifth ligand for a second Cu(II) ion bound to the macrocyclic tetramine **3**. For Cu1, the N_2S_2 coordination geometry is distorted square-planar as in ***rac*-2**, with some small, but significant differences. For example, the Cu1−S(bridging) distance (2.2586(11) Å) is 0.03−0.04 Å longer than the three Cu−S(terminal) distances in ***rac*-2** and ***rac*-5**. In addition, the tetrahedral twist angle in ***rac*-5** (16°) is about half as large as that in ***rac*-2** (33°). Cu(2) exhibits distorted square-pyramidal coordination with S2 apical, comparable to the coordination geometries in **13** and **14**.[6] The bridging S(thiolate) atoms in ***rac*-5**, **13**, and **14** exhibit pyramidal coordination with Cu(II)−S(thiolate)−Cu(II) angles of 116.18(4)°, 128.6(3)°, and 128.6(1)°, respectively. Last, the Cu2−S2 distance in ***rac*-5** (2.5329(11) Å) is ca. 0.06 Å longer than the average of the Cu−S(thiolate) distances in **13** and **14** (Table 3).

***rac*-6** consists formally of two ***rac*-2** and three Cu(I)Cl groups linked by bridging and doubly bridging thiolate ligands. It contains a crystallographically imposed 2-fold axis coincident with the Cu3−Cl1 bond; consequently, only one ***rac*-2** unit is crystallographically unique. Doubly bridging S2 ligates one Cu(II) atom and two Cu(I) atoms, while singly bridging S1 ligates one Cu(I) and one Cu(II) ion; as a result,

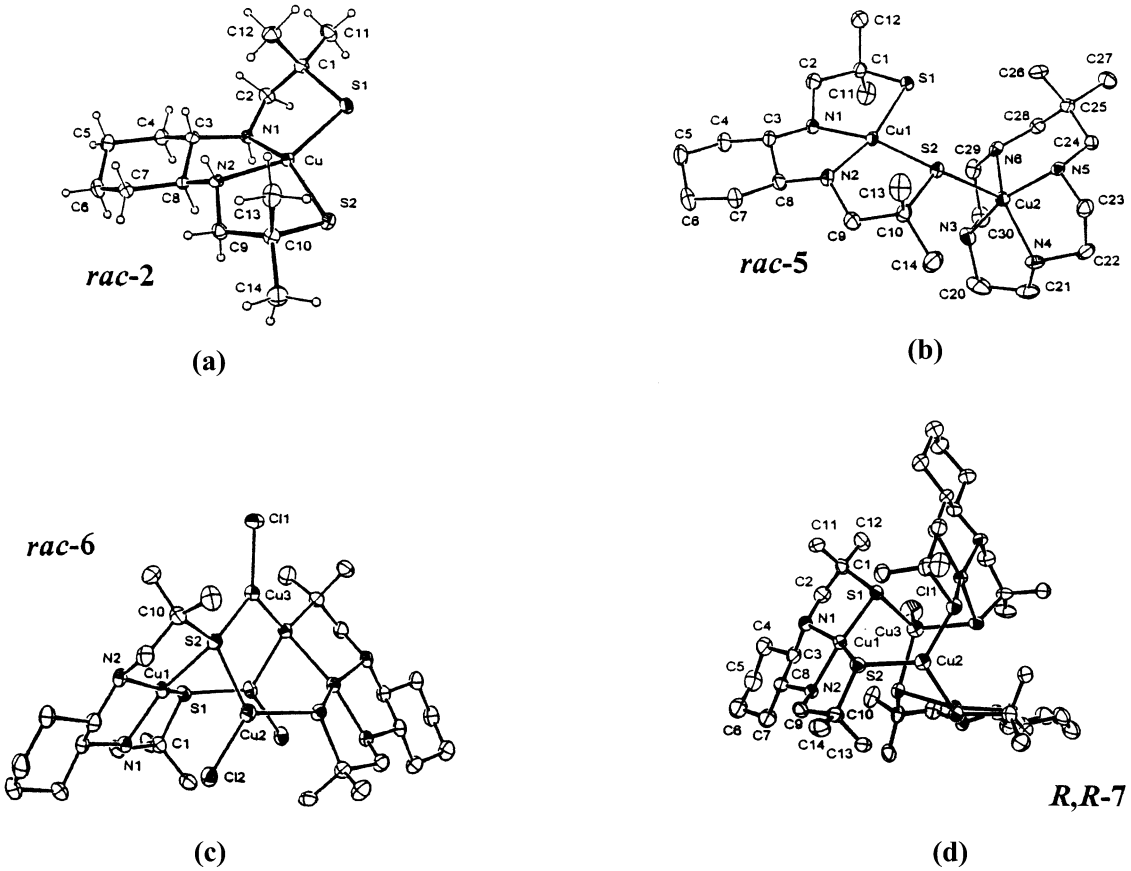

Figure 1. Views of (a) ***rac*-2**, (b) ***rac*-5**, (c) ***rac*-6**, and (d) ***R,R*-7** showing the atom-numbering schemes. Complex ***rac*-6** utilizes a crystallographic 2-fold axis passing through Cu3 and Cl1; cation ***R,R*-7** utilizes a crystallographic 3-fold axis passing through Cu2, Cu3, and Cl1.

Table 2. Metric Parameters for the Complexes Studied (Å, deg)[a]

	rac-**2**	***rac*-5**··2ClO_4	***rac*-6**·2DMF	***R,R*-7Cl**·solvate
Cu1−S1	2.2323(7)	2.2228(11)	2.2359(13)	2.263(3)
Cu1−S2	2.2308(8)	2.2586(11)	2.2595(14)	2.260(3)
Cu1−N1	2.043(2)	2.029(3)	1.996(4)	2.048(8)
Cu1−N2	2.048(2)	2.019(3)	2.016(3)	2.040(8)
Cu2−S2		2.5329(11)	2.2931(14)	
Cu2−N3, Cu2−S1′, Cu3−S2		2.007(4)	2.2136(13)	2.247(3)
Cu2−N4, Cu2−Cl2		2.041(3)	2.2287(14)	
Cu2−N5, Cu3−S2, Cu3−S1		2.032(3)	2.2132(13)	2.381(4)
Cu2−N6, Cu3−Cl1		2.056(3)	2.158(2)	2.352(6)
S1···S2	3.579(1)	3.4529(16)	3.507(2)	3.597(4)
Cu1···Cu2		4.0699(9)	2.8231(9)	3.5570(17)
Cu1···Cu3			3.9628(8)	3.3386(18)
S1−Cu−S2/N1−Cu−N2	32.76(6)	15.84(7)	25.8(2)	24.3(3)
S1−Cu1−S2	106.62(3)	100.79(4)	102.52(5)	105.36(11)
S1−Cu1−N1	88.85(6)	88.92(10)	88.94(11)	88.9(2)
S1−Cu1−N2	154.61(7)	164.74(11)	158.89(12)	162.1(3)
S2−Cu1−N1	152.63(6)	167.35(11)	160.03(11)	156.7(3)
S2−Cu1−N2	89.75(6)	87.90(10)	89.06(12)	87.4(3)
N1−Cu1−N2	84.57(8)	84.50(14)	85.51(15)	83.4(3)
N4−Cu2−N5, S2−Cu2−S1′		84.67(14)	112.50(5)	
N4−Cu2−N6, S2−Cu2−Cl2		145.88(14)	121.88(5)	
N5−Cu2−N6, S1′-Cu2−Cl2		96.22(13)	125.56(5)	
Cu1−S2−Cu2, S2−Cu3−Cl1		116.18(4)	125.73(3)	111.77(8)
S2−Cu3−S2′, S1−Cu3−S1′			108.54(7)	107.08(9)

[a] Symmetry transformation for ***rac*-6**·2DMF: $2-x, y, {}^1/_2 - z$; for ***R,R*-7Cl**, $1-z, x-{}^1/_2, {}^1/_2-y$.

the coordination geometry of S1 is pyramidal, while that of S2 is distorted tetrahedral. The resulting $Cu_5S_4N_4Cl_3$ core contains alternating copper and sulfur atoms with the connectivity of the carbon atoms in bicyclo[3.3.1]nonane (Figure 2a). $M_5S_4N_4X_3$ connectivity has been observed in $[Ni(II)(\mathbf{1})]_2[Cu(I)I]_3$[22] and **15**,[8] each of which contain M(II)-N_2(amine)S_2(thiolate) [M(II) = Ni(II),[22] Cu(II)[8]] units bridged by Cu(I)X (X = I,[22] Cl[8]) groups.

The Cu(II) atoms in ***rac*-6** have a distorted square-planar coordination geometry similar to those in ***rac*-2**, ***rac*-5**, and

(22) Fox, S.; Stibrany, R, T.; Potenza, J. A.; Schugar, H. J. *Acta Crystallogr.* **1996**, *C52*, 2731−2734.

Chart 1

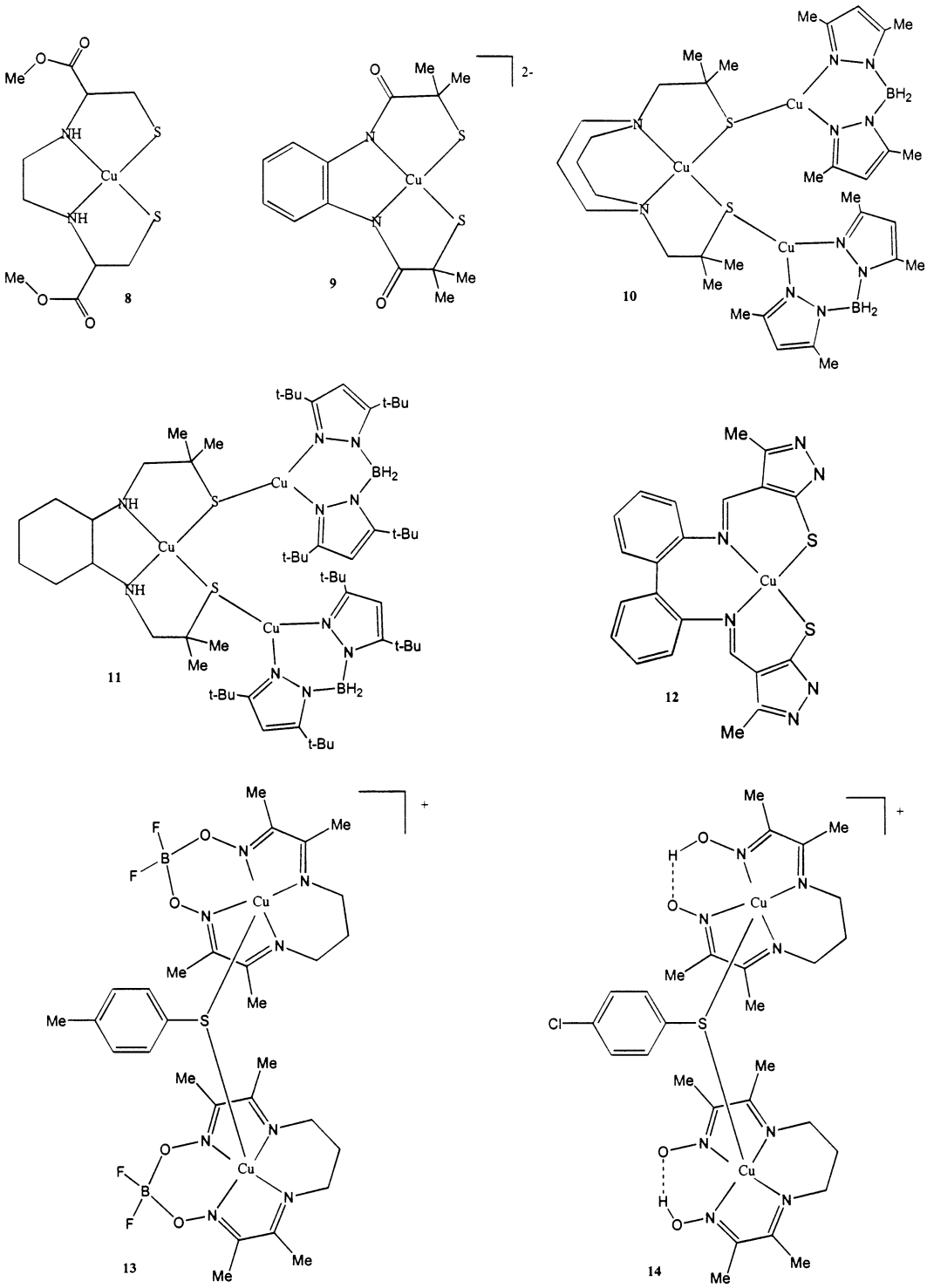

***R,R*-7** (Table 2). The Cu1···Cu2 distance [2.8231(9) Å] is short compared with that in **15** [2.943 Å], raising the possibility of a copper−copper bonding interaction, either directly or via the bridging thiolate, S2. Such an interaction might be expected to lead to changes in the Cu1 coordination geometry, but only small changes are observed. If a Cu1−Cu2 interaction is absent in ***rac*-6**, the Cu(I) atoms exhibit distorted trigonal-planar S_2(thiolate)Cl coordination geometries with metal−ligand distances for Cu2 longer than those for Cu3 (Figure 3). Relatively long Cu2−Cl2 and Cu2−S2 bond lengths are consistent with Cu1 acting as a fourth ligand for Cu2 and with a weak Cu1−Cu2 interaction. In this view, the Cu2−Cl2 and Cu2−S2 bond lengths increase with the Cu2 coordination number, as expected for an ion with a spherically symmetric valence shell. If Cu1 is considered to ligate Cu2, the Cu2 coordination geometry is best described as highly distorted trigonal-pyramid.

Cu_2^{3+} units are relatively rare, although the number of examples containing delocalized average-valence Cu(1.5)−Cu(1.5) bonds has been increasing in recent years.[23] In the

Table 3. Metric Parameters for Selected Species Containing Cu(II)(*cis*-N_2S_2) Units (distances in Å and angles in deg)

	8	**9**	**10**	**11**	**12**	**13**	**14**
Cu−S[a]	2.230(5) 2.262(4)	2.2381(8) 2.243(1)	2.247(3)	2.260(9)	2.245(1)	2.506(7) 2.436(7)	2.484(2) 2.459(3)
Cu−N	2.002(11) 2.059(13)	1.962(2) 1.963(2)	2.019(8)	2.020	1.984(3)	1.93(2) to 2.01(2)[b]	1.955(6) to 1.982(5)[b]
S−Cu−S/N−Cu−N	21.0(7)	planar	34(1)	36(1)	51.9		
S1···S2	3.406(6)	3.439	3.432	3.662	3.105(2)		
S1−Cu−S2	98.6(2)	100.27(3)	99.5(2)	108.12	87.5(1)	128.6(3)	128.6(1)
reference	2a	19	7	7	20	6	6

	15	**19**[c]	**24**
Cu−S	2.234(2) 2.267(2)	2.250(1) 2.292(1)	2.237(5) to 2.266(4)
Cu−N	2.006(5) 2.011(5)	2.115(3) 2.125(3)	1.965(12) to 2.055(11)
S−Cu−S/N−Cu−N			18.2 to 20.5[d]
S1···S2	3.482	3.480(2)	3.451(6) to 3.497(6)
S1−Cu−S2	101.3(1)	99.64(3)	99.8(2) to 102.2(2)
Cu···Cu	2.943	2.9306(9)	2.946(3) to 3.532(2)[e]
reference	8	24	5a

[a] Cu = Cu(II) unless otherwise noted. [b] Range for eight Cu−N(imine) distances. [c] For **19**, Cu = Cu(1.5) [d] S1−Cu−N1/S2−Cu−N2 dihedral angles [e] Cu(I)···Cu(II) distances.

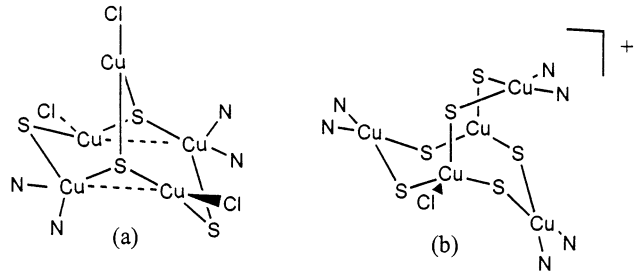

Figure 2. (a) Sketch of the $Cu_5S_4N_4Cl_3$ core in ***rac*-6**. (b) Sketch of the $Cu_5S_6N_6Cl^+$ core in ***R,R*-7**.

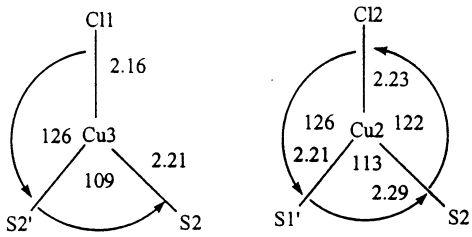

Figure 3. Comparison of the metric parameters for the Cu(I)S_2(thiolate)-Cl units in ***rac*-6**. Distances and angles are approximated to three significant figures.

first example reported, two copper ions were forced into proximity by constraints imposed by the macrobicyclic octaaza ligands **16**−**18** (Chart 2). The copper ions exhibit trigonal-bipyramidal CuN_4Cu coordination with Cu−Cu bond distances ranging from 2.364(2) Å[23b] in $[Cu_2\mathbf{17}]^{3+}$ to 2.419(1) Å[23c] in $[Cu_2\mathbf{18}]^{3+}$. Spectroscopic data support the view that these species contain σ-bonded, average-valence Cu_2^{3+} units unsupported by bridging ligands.[23d] A delocalized thiolate-bridged mixed-valence Cu_2^{3+} cation **19**, with distorted trigonal-pyramidal coordination geometry, has also been characterized structurally (Cu−Cu, 2.9306(9) Å) and spectroscopically.[24] Last, direct Cu(1.5)−Cu(1.5) bonding has been reported for several mixed-valence copper complexes (**20**−**22**) containing oxygen-donor ligands.[23e,f] These species exhibit $Cu(O_4Cu)$ distorted square-pyramidal coordination geometries with Cu−Cu distances ranging from 2.3988(8) to 2.4246(12) Å. The Cu1−Cu2 distance in ***rac*-6** is ca. 0.4 Å longer than those in the Cu_2^{3+} complexes with copper ions in direct contact, yet shorter by about 0.1 Å than the Cu−Cu contact in the thiolate-bridged cation **19**. However, in ***rac*-6**, the coordination geometries of Cu1 and Cu2 are clearly those of Cu(II) and Cu(I), respectively, with perhaps modest expansion of the Cu2 coordination sphere. Taken together, these data suggest a valence-trapped system for ***rac*-6** with the possibility of a weak Cu···Cu interaction, either directly or via the bridging thiolate ligand.

The chemistry associated with the formation of ***rac*-6** requires some comment. ***rac*-6** was initially synthesized serendipitously by the reaction of $CuCl_2$ and ***rac*-2**. Our intent was to prepare a trinuclear complex with two ***rac*-2** units bound to a Cu(II) ion via four bridging thiolates, similar to the known Ni(II) analogue **25**.[25a] Appearance of Cu(I) in the product required oxidation of some substance in the reaction mixture, most likely ***rac*-2**. Once the composition of ***rac*-6** was established, we attempted a rational synthesis using ***rac*-2** and CuCl as reactants. This led directly to ***rac*-6**.

(23) (a) Harding, C.; McKee, V.; Nelson, J. *J. Am. Chem. Soc.* **1991**, *113*, 9684−9685. (b) Barr, M. E.; Smith, P. H.; Antholine, W. E.; Spencer, B. *J. Chem. Soc., Chem. Commun.* **1993**, 1649−1652. (c) Farrar, J. A.; McKee, V.; Al-Obaidi, A. H. R.; McGarvey, J. J.; Nelson, J.; Thomson, A. J. *Inorg. Chem.* **1995**, *34*, 1302−1303. (d) Al-Obaidi, A.; Baranovič, G.; Coyle, J.; Coates, C. G.; McGarvey, J. J.; McKee, V.; Nelson, J. *Inorg. Chem.* **1998**, *37*, 3567−3574. (e) LeCloux, D. D.; Davydov, R.; Lippard, S. J. *J. Am. Chem. Soc.* **1998**, *120*, 6810−6811. (f) LeCloux, D. D.; Davydov, R.; Lippard, S. J. *Inorg. Chem.* **1998**, *37*, 6814−6826.

(24) Houser, R. P.; Young, V. G.; Tolman, W. B. *J. Am. Chem. Soc.* **1996**, *118*, 2101−2102.

(25) (a) Farmer, P. J.; Solouki, T.; Molls, D. K.; Soma, T.; Russell, D. H.; Reibenspeis, J. H.; Darensbourg, M. Y. *J. Am. Chem. Soc.* **1992**, *114*, 4601−4605. (b) Tuntulani, T.; Reibenspies, J. H.; Farmer, P. J.; Darensbourg, M. Y. *Inorg. Chem.* **1992**, *31*, 3497−3499. (c) Lyon, E. J.; Musie, G.; Reibenspies, J. H.; Darensbourg, M. Y. *Inorg. Chem.* **1998**, *37*, 6942−6946.

Chart 2

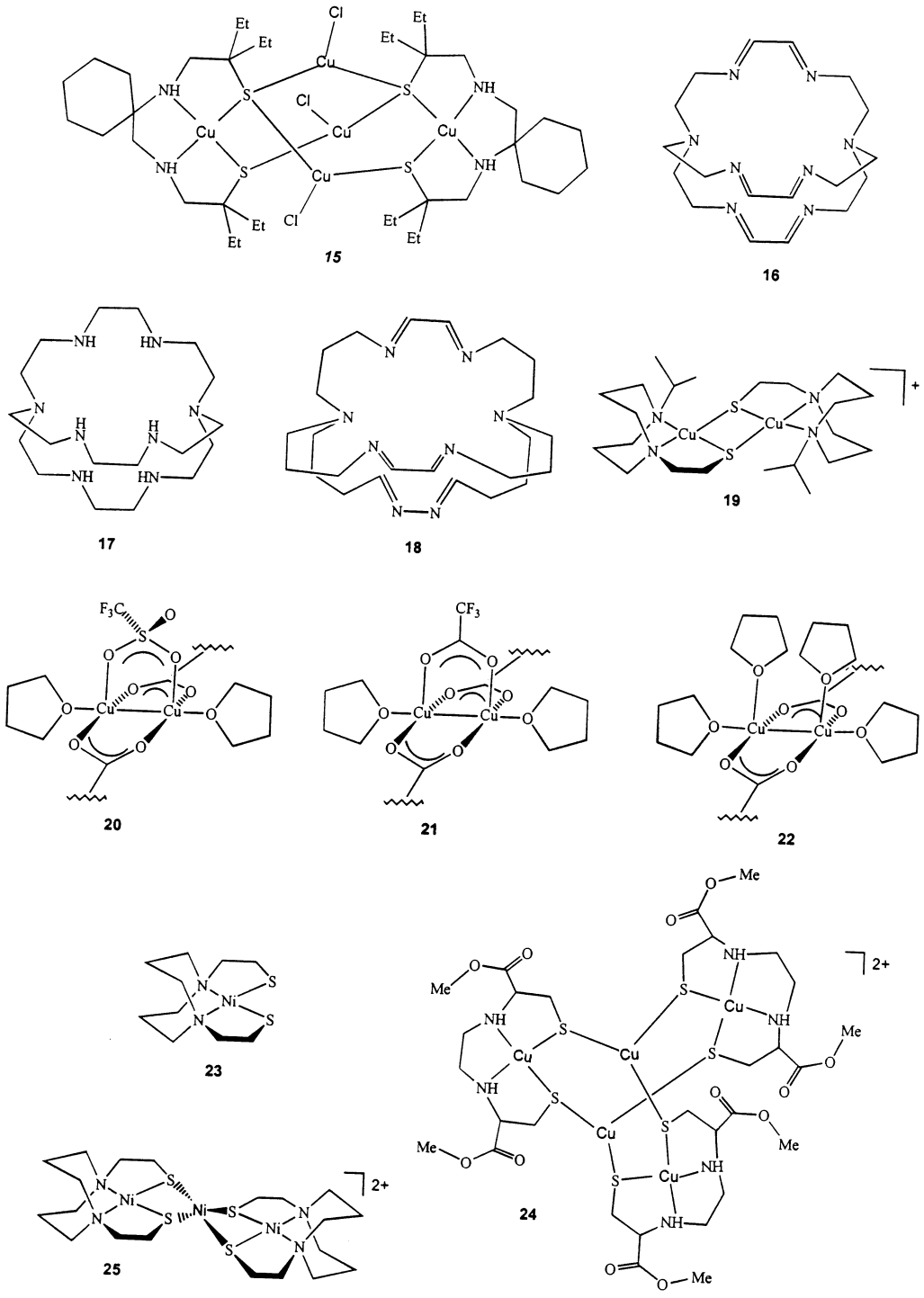

Finally, to help assign the electronic spectra of these pentanuclear clusters, we attempted to prepare the mixed-metal complex Zn(***rac*-1**)$_2$(CuCl)$_3$ directly from Zn(***rac*-1**) and CuCl. Only the zinc-free product ***rac*-6** was isolated, as evidenced by its color, electronic spectrum, crystal morphology, cell dimensions, and X-ray fluorescence spectrum, which showed that Zn was not present in the product. Disproportionation of Cu(I), along with displacement of Zn(II) by Cu(II), nominally is required for this product to form. Owing to the greater affinity of Cu(II) relative to Zn(II) for N,S-donor ligands, displacement of Zn(II) is not unexpected in the presence of Cu(II). The *indirect* syntheses noted above, both of which require copper redox reactions, as well as the direct preparation, all yield the basic $Cu_5S_4N_4Cl_3$ mixed-valence pentanuclear core in Figure 2a, suggesting that a substantial thermodynamic stability of this unit helps drive the redox processes.

***R,R*-7** contains three ***R,R*-2** units linked by singly bridging thiolate ligands to a Cu(I) ion and Cu(I)Cl group (Figure 1d). The cation contains a crystallographically required 3-fold axis coincident with the Cu3−Cl1 bond and passing through Cu2. There is one unique ***rac*-2** unit, and each ***rac*-2** sulfur

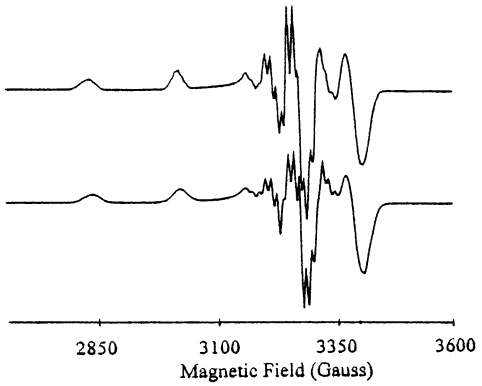

Figure 4. Observed (top) and simulated[26] (bottom) X-band EPR spectra of ***rac*-2** (14 mmol, glassed acetonitrile, 80 K).

atom singly bridges one Cu(I) and one Cu(II) ion to form a pentanuclear cluster, which is completed by chloride ligation of *one* of the Cu(I) ions. The resulting $Cu_5S_6N_6Cl$ core contains alternating copper and sulfur atoms with the connectivity of the carbon atoms in bicyclo[3.3.3]undecane (Figure 2b), a connectivity observed previously for alternating metal and sulfur atoms in **24** (**[(8)**$_3$**Cu**$_2$**]**$^{2+}$**(ClO**$_4$**)**$_2$**)**[5a] and in a Ni(II)/Zn(II) analogue **26** ([**23**]$_3$(ZnCl)$_2$]$^{2+}$).[25b] These complexes can also be viewed[25b] as containing a trigonal-bipyramid of metal ions decorated by three N_2S_2 ligands and zero (**24**), one (***R,R*-7**), or two (**26**) chloride anions. The axial metal ions, Cu(I) or Zn(II), exhibit trigonal or tetrahedral coordination depending on the absence or presence of a chloride ligand. The Cu(I)···Cu(I) distance in ***R,R*-7** (3.923(3) Å) corresponds to axial···axial separation in the Cu_5 trigonal-bipyramid and is substantially longer than the corresponding distance in **24** (3.016(3) Å). In contrast, the equatorial Cu(II)···Cu(II) distances show a much smaller variation (4.876(3)−5.024(3) Å). Viewed this way, the dication in **24** is axially compressed compared with the monocation ***R,R*-7**.

Magnetic Studies. Polycrystalline ***rac*-2** exhibits an effective magnetic moment of 1.95(2) μ_B/mol at 25 °C, a value appropriate for a mononuclear Cu(II) species. EPR spectra of ***rac*-2** (Figure 4) are nearly identical to those reported for the chiral analogue **8**, except that the nitrogen superhyperfine (SHF) splitting in **8** is less well resolved.[2a] Both complexes have axial EPR spectra typical for tetragonal Cu(II) chromophores with a $d_{x^2-y^2}$ ground state. The ***rac*-2** spectrum was fit with $g_{\|}(Cu) = 2.113$, $g_{\perp}(Cu) = 2.018$, $A_{\|}(Cu) = 176 \times 10^{-4}$ cm^{-1}, $A_{\perp}(Cu) = 40.1 \times 10^{-4}$ cm^{-1}, $A_{\|}(N) = 7.0 \times 10^{-4}$ cm^{-1}, and $A_{\perp}(N) = 11.3 \times 10^{-4}$ cm^{-1}. As probed by the g values and Cu SHF coupling constants, the presence of two aliphatic thiolate ligands appears to have little effect on the ground state electronic structure of these approximately planar Cu(II) chromophores. These results are in sharp contrast to the type 1 blue copper protein active sites for which substantial Cu−S covalency results in striking electronic spectral and magnetic effects.[27]

(26) Simulations were performed using the program QPOWA obtained from Prof. R. L. Belford, Illinois ESR Research Center, 506 S. Matthews St., Urbana, IL 61801.

(27) Solomon, E. I.; Baldwin, M. J.; Lowery, M. D. *Chem. Rev.* **1992**, *92*, 521−542.

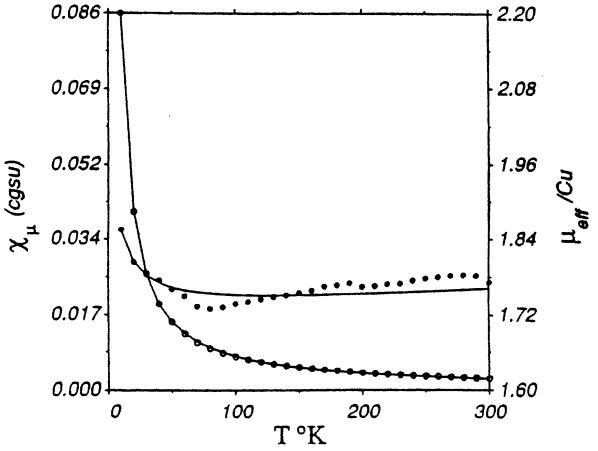

Figure 5. Magnetic susceptibility and effective magnetic moment of ***rac*-5** as a function of temperature.

The magnetochemical behavior of polycrystalline ***rac*-5**·$2ClO_4$ is shown in Figure 5. Isolated, approximately square-pyramidal Cu(II) species exhibit axial EPR spectra which can be interpreted by assuming that the half-occupied Cu(II) orbital is located in the molecular "*xy*" plane approximately orthogonal to the σ-bonding lone pair supplied by the weakly bound apical ligand on the "*z*" axis. The substantial antiferromagnetism commonly exhibited by ligand-bridged dinuclear Cu(II) complexes is strongly attenuated when, as in the case of ***rac*-5**, superexchange must proceed through a single apical bond. In ***rac*-5** then, antiferromagnetic coupling is expected to be strongly attenuated both by the weakness of the long apical Cu−S bonds and by the approximately orthogonal orbital interaction of the bridging thiolate lone pair with the Cu(II) d-vacancy. Under these circumstances, a weak ferromagnetism can prevail.[28] Least-squares analysis of the susceptibility data suggests that the system can be reasonably modeled using an effective g value in the range 1.96−1.99, a J value in the range 2.5 to 5 cm^{-1}, and intermolecular interactions between the dinuclear complexes (zJ) in the range −0.25 to +0.19 cm^{-1}. Some degree of intramolecular spin−spin interaction between the two Cu(II) centers is also apparent from the EPR data. Spectra measured in noncoordinating solvents consist of a single broad absorption centered at about $g = 2.05$. ***rac*-5** is cleaved by coordinating solvents such as methanol, in which the observed EPR spectra (not shown) are the sum of the absorptions from isolated *cis*-Cu(II)N_2S_2 and Cu(II)N_4 monomers. A weak signal at about 1500 G in the X-band EPR spectrum of the thiolate-bridged Cu(II)cyclops system **14** was assigned as a $\Delta M = \pm 2$ transition, implying some interaction between the Cu(II) ions in that system as well.[6a]

***rac*-6** contains two *cis*-Cu(II)N_2S_2 subunits bridged by three Cu(I)Cl fragments. Our magnetochemical study of the related complex **24** revealed only weak ferromagnetic coupling ($J = 0.26$ cm^{-1}). The weak magnetic coupling anticipated for ***rac*-6** was not quantified.

(28) Hathaway, B. J. In *Comprehensive Coordination Chemistry*; Wilkinson, G., Gillard, R. D., McCleverty, J. A., Eds.; Permagon Press: New York, 1987; Vol. 5, pp 657−662.

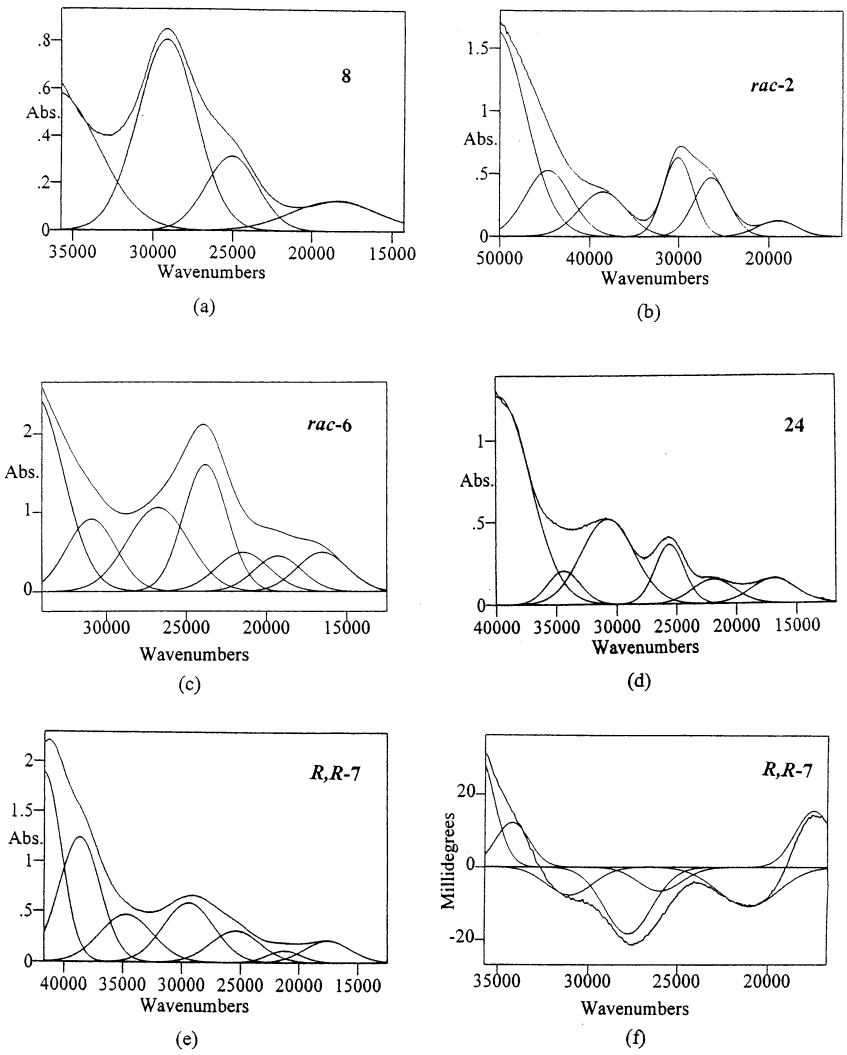

Figure 6. Electronic spectra and deconvoluted spectra of (a) **8**, measured at RT as a 2.79×10^{-3} M solution in DMF having a path length of 0.1 cm, (b) ***rac*-2**, measured at RT as a 1.25×10^{-3} M solution in acetonitrile having a path length of 0.1 cm, (c) ***rac*-6**, measured at RT as a 0.459×10^{-3} M (0.917×10^{-3} M in Cu(II)) solution in DMF having a path length of 0.1 cm, (d) **24**, measured at 80 K as a 0.506×10^{-3} M (1.52×10^{-3} in Cu(II)) solution in a glassed DMF/glycerol solution having a path length of 0.17 cm, and (e) ***R,R*-7**, measured at RT as a 0.938×10^{-4} M (2.82×10^{-3} M in Cu(II)) solution in methanol having a path length of 0.1 cm. (f) CD spectrum of a 0.938×10^{-4} M solution of ***R,R*-7Cl** in methanol having a path length of 0.1 cm.

Electrochemistry for *rac*-2. For ***rac*-2**, the Cu(I)/Cu(II) couple at −0.51 V vs NHE is reversible and nearly independent of scan rates from 20 to 100 mV/s. Presumably owing to its dithiolate ligation and approximately planar geometry, both of which preferentially stabilize the Cu(II) state, ***rac*-2** shows a substantially lower redox potential than the type 1 copper proteins (0.187−0.780 V vs NHE).[29] It is also lower than those from approximately trigonal Cu(II)-N_2S(thiolate) chromophores designed to mimic type 1 copper sites (approximately −0.12 V vs NHE),[12a] but is comparable to those reported (−0.5 to −0.9 V vs NHE) for nearly planar Cu(II)N_2S_2(thiopyrazolone) complexes.[30]

Electronic Spectral Studies. Electronic spectra are shown in Figure 6 and summarized in Table 4; spectra of **8** and **24** have been included to facilitate interpretations. Mononuclear **8** (Figure 6a) shows a LF absorption centered at 18 600 cm^{-1} along with more intense higher-energy absorptions at 25 000, 29 100, and >36 100 cm^{-1}, which we assign respectively to π (S) →, σ(S) →, and π (S,C) → Cu(II) LMCT. We believe that the latter absorption is too low in energy to result from σ(N) → Cu(II) LMCT,[31] but that it may result from LMCT originating from a relatively stable thiolate lone pair that has considerable carbon character (see below). Absorption measurements at higher energies were precluded by the insolubility of **8** in solvents less polar than DMF. Deconvoluted spectra of ***rac*-2** (Figure 6b) show a LF absorption centered at 19 000 cm^{-1}, along with more intense higher energy absorptions at 26 400, 30 100, 38 500, 44 600, and 50 500 cm^{-1}, which we assign respectively to π (S) →, σ(S) →, π (S,C) →, σ(N) → Cu(II) LMCT, and overlapping amine and thiolate Rydberg absorptions.[4a]

The Cu−S−C bond angles in ***rac*-2** and in **8** [range 94.30(8)−97.0(5)°] imply that the orientation of the Cu−

(29) Battistuzzi, G.; Borsari, M.; Loschi, L.; Righi, F.; Sola, M. *J. Am. Chem. Soc.* **1999**, *121*, 501−506.
(30) Knoblauch, S.; Benedix, R.; Ecke, M.; Gelbrich, T.; Sieler, J.; Somoza, F.; Hennig, H. *Eur. J. Inorg. Chem.* **1999**, 1393−1403.
(31) Kennedy, B. P.; Lever, A. B. P. *J. Am. Chem. Soc.* **1973**, *95*, 6907−6913.

Table 4. Summary of Deconvoluted Electronic Spectra

	solution UV/vis				solution CD	
system	energy (cm^{-1})	ϵ per Cu(II)[f]	assignment 1	assignment 2	cm^{-1}	deg $\times 10^{-3}$
8[a]	18 600	450	LF			
	25 000	1100	π(S) → Cu(II) LMCT			
	29 100	2900	σ(S) → Cu(II) LMCT			
	>36 100	>2100	π(S,C)→Cu(II) LMCT			
***rac*-2**[b]	19 000	990	LF			
	26 400	3700	π(S) → Cu(II) LMCT			
	30 100	5000	σ(S) → Cu(II) LMCT			
	38 500	2800	π(S,C) → Cu(II) LMCT			
	44 600	4200	σ(N) → Cu(II) LMCT			
	50 500	13 000	S,N Rydberg			
***rac*-6**[c]	16 500	540	LF			
	19 300	490	Cu(I) → Cu(II) MMCT			
	21 500	540	$\pi(S_P)$ → Cu(II) LMCT			
	23 800	1800	$\sigma(S_P)$ → Cu(II) LMCT + $\pi(S_T)$ → Cu(II) LMCT			
	26 800	1200	$\sigma(S_T)$ → Cu(II) LMCT			
	30 900	1000	Cu(I) → $S_{P,T}$ MLCT			
	34 500	2800	Cu(I) → $S_{P,T}$ MLCT			
24[d]	16 900	580	LF	same as 1		
	21 900	570	Cu(I) → Cu(II) MMCT	π(S) → Cu(II) LMCT		
	25 600	1400	π(S) → Cu(II) LMCT	σ(S) → Cu(II) LMCT		
	30 700	2000	σ(S) → Cu(II) LMCT	Cu(I) → S MLCT		
	34 400	800	Cu(I) → S MLCT	same as 1		
	39 800	4900	σ(N) → Cu(II) LMCT + π(S,C) → Cu(II)LMCT	same as 1		
***R,R*-7**[e]	17 400	700	LF	same as 1	17 400	+15.8
	21 600	500	Cu(I) → Cu(II) MMCT	π(S) → Cu(II) LMCT	21 000	−10.8
	26 000	1100	π(S) → Cu(II) LMCT	σ(S) → Cu(II) LMCT	27 400	−21.
	29 600	2100	σ(S) → Cu(II) LMCT	Cu(I) → S MLCT	31 300	−7.2
	35 000	1800	Cu(I) → S MLCT	same as 1	34 500	+14.5
	38 300	3500	Cu(I) → S,Cl MLCT + π(S,C) → Cu(II) LMCT	same as 1	>36 000	>20.
	41 500	7500	σ(N) → Cu(II) LMCT	same as 1		

[a] Measured in DMF at RT; ref 2a. [b] Measured in acetonitrile at RT. [c] Measured in DMF at RT. [d] Measured in glassed glycerol at 80 K. [e] Measured in methanol at RT. [f] For convenience, ϵ values are reported per Cu(II) even though some of the assignments are attributed to the Cu(I) ions in the pentanuclear species.

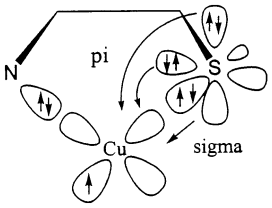

Figure 7. Sketch of a Cu(II)N(amine)S(thiolate) chromophore as found in ***rac*-2** and **8** showing the interaction of the sulfur and nitrogen valence-shell orbitals with the Cu(II) d-vacancy.

S(thiolate) bonds relative to the Cu(II) $d_{x^2-y^2}$ vacancy is consistent with the conventional metal−thiolate bonding view in which Cu(II)−S bonding consists of one σ- and two nondegenerate π-bonding interactions (Figure 7).[32] This arrangement results in typical EPR spectra (see above) and the appearance of a π (S) → Cu(II) LMCT absorption flanked at higher energy by a more intense σ(S) → Cu(II) LMCT absorption. Molecular orbital calculations[27] suggest that the three sulfur lone pairs are not degenerate in free thiolate, but that one exhibits considerable S−C bonding character and is more stable by about 2 eV than the other two. The relatively high binding energy and reduced spatial extension of this orbital is expected to result in LMCT absorption for **8** and ***rac*-2** that is relatively weak and shifted as much as 16 000 cm^{-1} toward higher energy from those noted above (25 000 to 30 100 cm^{-1}). Such absorptions could be obscured by the strong σ(N) → Cu(II) LMCT band centered at 44 600 cm^{-1}, an assignment based on published results for a series of Cu(II)N_4 chromophores.[31] However, the absorption of ***rac*-2** at 38 500 cm^{-1} appears at an energy intermediate between that appropriate for π(S), σ(S) → Cu(II) LMCT and σ(N) → Cu(II) LMCT absorptions and may arise from π(S,C) → Cu(II) LMCT, the third possible thiolate LMCT absorption.

Prior assignments of σ(S) → and the weaker π(S) → Cu(II) LMCT in **8** were supported by CD measurements.[4b] The Kuhn factor ($\Delta\epsilon/\epsilon$) of the absorption at 25 000 cm^{-1} in **8** is about 4 times larger than that of the stronger absorption at 29 100 cm^{-1}. LMCT absorption from the relatively strong metal−ligand σ-interaction affords linear charge displacement and characteristic electric dipole allowedness. In contrast, that from the weaker metal−ligand π-interaction has less dipole allowedness but requires linear plus rotary charge displacement (Figure 7). This gives rise to greater

(32) Shadle, S. E.; Penner-Hahn, J. E.; Schugar, H. J.; Hedman, B.; Hodgson, K. O.; Solomon, E. I *J. Am. Chem. Soc.* **1993**, *115*, 767−776.

CD allowedness and a larger $\Delta\epsilon$. Thus, the larger $\Delta\epsilon$ and smaller ϵ of the π(S) → Cu(II) LMCT are expected to result in a larger Kuhn factor than that of the flanking σ (S) → Cu(II) LMCT absorption.

While we are confident of the spectral assignments of **8** and ***rac*-2**, a similar situation does not prevail for ***rac*-6**, **24**, and ***R,R*-7**, whose spectra are enriched by interactions arising from the bridging Cu(I) ions and the mononuclear units. Additional structural features associated with these pentanuclear complexes include singly and doubly bridging thiolates, three- and four-coordinated Cu(I) ions, varying Cu(I) ligand sets, and the possibility of Cu(I)···Cu(II) intervalence absorptions either via bridging thiolates or directly through space. These features are expected to extend the types and complexities of electronic absorptions significantly. Indeed, the UV−vis spectra of ***rac*-6**, **24**, and ***R,R*-7** exhibit multiple overlapping absorptions over the entire visible and ultraviolet spectral regions studied.

Although many polynuclear Cu(I)−S(thiolate) complexes have been characterized crystallographically, we are aware of only a few electronic spectroscopic studies. A *colorless* complex[33] containing a linear aliphatic S(thiolate)−Cu(I)−S(thiolate) chromophore exhibits absorption at 39 500 cm^{-1}, assigned as Cu(I) → S MLCT. A second, *yellow* Cu(I) complex of the same ligand contains three linear S_2(thiolate)-Cu(I) and two trigonal aliphatic S_3(thiolate)Cu(I) chromophores; absorptions at 36 600 and 33 300(sh) cm^{-1} were assigned respectively as Cu(I) → S(linear) and Cu(I) → S(trigonal) MLCT.[33]

The effects of coordination by soft metal ions such as Cu(I) on thiolate → metal LMCT absorptions are not well known. We are aware of only one example, the thiolate group of $Co(en)_2(NH_2CH_2CH_2S)^{2+}$, which can also coordinate added soft metal ions.[34] Coordination of Ag^+ (linear S(thiolate)−Ag−S(thiolate) units), Cu^+ (bridging $Cu(I)_2S(thiolate)_2$ units), and CH_3Hg^+ changed the position and intensity of the S → Co(III) LMCT absorptions only modestly.[34,35] It is likely that comparable spectroscopic results are obtained for the effect of bridging Cu(I) on the S → Cu(II) LMCT absorptions in our complexes.

With this background, we consider the electronic spectra of the pentanuclear complexes. Each shows a LF absorption (range 16 500−17 400 cm^{-1}) red-shifted from the corresponding monomer bands, in agreement with the expectation that Cu(I) coordination lowers thiolate basicity and ligand-field strength. Bands at 39 800 cm^{-1} (**24**) and 41 500 cm^{-1} (***R,R*-7**) are assigned as σ(N) → Cu(II) LMCT, consistent with the position of a similar absorption for ***rac*-2**. Absorptions thought to result from π(S,C) → Cu(II) LMCT shown by ***rac*-2** at 38 500 cm^{-1} and by ***R,R*-7** at 38 300 cm^{-1} may also contribute to the σ(N) → Cu(II) LMCT absorption of **24**. Solubility limitations and solvent cutoff precluded spectral data acquisition at high enough energy to observe a comparable band in ***rac*-6**.

We see two plausible assignments for the intermediate-energy absorptions in **24** and ***R,R*-7** (Table 4). Assignment 1 assumes that the positions of π(S) → and σ(S) → Cu(II) LMCT bands are little changed from those of the mononuclear complexes and that any remaining higher-energy absorptions are due to Cu(I) → S MLCT, Cu(I) → Cl MLCT (where appropriate), π(S,C) → Cu(II) LMCT, and σ(N) → Cu(II) LMCT. In **24**, both Cu(I) ions are coordinated to three thiolates; therefore, on the basis of the discussion above, the absorption at 34 400 cm^{-1} is assigned to Cu(I) → S MLCT. By analogy, the band at 35 000 cm^{-1} in ***R,R*-7** is similarly assigned. The higher-energy absorption at 38 300 cm^{-1} in ***R,R*-7** might then be due to Cu(I) → S MLCT, Cu(I) → Cl MLCT, π(S,C) → Cu(II) LMCT, or a combination of all three.

Assignment 2 assumes that the weaker ligand field at Cu(II) in the pentanuclear complexes lowers the copper d-vacancy energy and red-shifts their Cu(II) LMCT bands from those in ***rac*-2**. For this assignment, Cu(I) → Cu(II) MMCT absorptions are assumed to be too weak in **24** and ***R,R*-7** to be observed in the presence of other absorptions in the vicinity of 21 000 cm^{-1}. For ***R,R*-7**, however, this assignment is inconsistent with the CD results (Table 4). The Kuhn factors for the CD absorptions at about 27 400 and 31 300 cm^{-1} are consistent with π and σ charge-transfer character, respectively. The electronic spectrum shows that the band at approximately 26 000 cm^{-1} has an ϵ value about half that of the band at 29 600 cm^{-1}. In contrast, the CD spectrum shows that the $\Delta\epsilon$ values for the corresponding pair of absorptions (27 600 and 31 300 cm^{-1}) are in an approximate 3:1 ratio (the $\Delta\epsilon$ values are proportional to the observed rotations). This results in an apparent ratio of Kuhn factors ($\Delta\epsilon/\epsilon$) for these absorptions of 5.64, consistent with the value observed for **8**.[2a] Regarding assignment 2, ϵ for the absorption at 21 600 cm^{-1} again is about half that of the absorption at 26 000 cm^{-1}, but $\Delta\epsilon$ for the corresponding CD absorption at 21 600 cm^{-1} is also considerably smaller than that of the absorption at 27 400 cm^{-1}. This gives a ratio of Kuhn factors of about 1.0, a value incompatible with their assignment as π(S) → and σ(S) → Cu(II) LMCT, respectively.

To complete assignment 2, bands at higher energies are assumed to arise from Cu(I) → S MLCT, Cu(I) → Cl MLCT, and σ(N) → Cu(II) LMCT. In **24**, which has no chloride ligands, the bands at 30 700 and 34 400 cm^{-1} are most reasonably assigned as Cu(I) → S MLCT. By analogy, the bands at 29 600 and 35 000 cm^{-1} in ***R,R*-7** are similarly assigned. The additional absorption shown by ***R,R*-7** at 38 300 cm^{-1} may originate from Cu(I) → Cl MLCT and/or π(S,C) → Cu(II) LMCT.

The absorption at ∼21 000 cm^{-1} in each pentanuclear spectrum is not shown by either reference mononuclear complex (***rac*-2** or **8**). It is too high for a $Cu(II)N_2S_2$ LF absorption and probably not high enough to be accounted for by π(S) → Cu(II) LMCT. The presence of Cu(II)−S(thiolate)−Cu(I) units in ***R,R*-7**, **24**, and ***rac*-6** suggests the

(33) Fujisawa, K.; Imai, S.; Kitajima, N.; Moro-oka, Y. *Inorg. Chem.* **1998**, *37*, 168−169.
(34) Heeg, M. J.; Elder, R. C.; Deutsch, E. *Inorg. Chem.* **1979**, *18*, 2036−2039.
(35) Lane, R. H.; Pantaleo, N. S.; Farr, J. K.; Coney, W. M.; Newton, M. G. *J. Am. Chem. Soc.* **1978**, *100*, 1610−1611.

possibility of intervalence absorptions (Cu(I) → Cu(II) MMCT) for these bands. Examples of intense visible and infrared Cu(I) → Cu(II) MMCT absorptions shown by binuclear mixed-valence copper complexes have been summarized recently.[23e] The high intensities of these absorptions require substantial electronic coupling between the Cu(I) and Cu(II) centers, a requirement supported by the observation of delocalized EPR spectra and by electronic structure calculations. A recent study of a more weakly coupled Cu(I)−Cl−Cu(II) chromophore having type 1 (localized) valences suggested that Cu(I) → Cu(II) MMCT accounted in part for electronic spectral changes relative to a reference Cu(II) monomer.[36] The greater covalency of thiolate compared with chloride implies that the potential for Cu(I) → Cu(II) MMCT in a Cu(I)−S−Cu(II) dinuclear unit should be better than that for a chloride-bridged unit.

In contrast to ***R,R*-7** and **24**, half the thiolates in ***rac*-6** exhibit pyramidal (S_P) coordination while the other half are coordinated tetrahedrally (S_T). These differences are expected to split the π(S) and σ(S) → Cu(II) LMCT absorptions, leading to a maximum of four bands instead of two. The LF absorption of ***rac*-6** at 16 500 cm^{-1} is the most red-shifted of the complexes in Table 4, and we expect concomitant shifts of the several types of charge-transfer absorptions. On this basis, we assign the absorption at 19 300 cm^{-1} as Cu(I) → Cu(II) MMCT red-shifted from its counterparts in **24** and ***R,R*-7**. We expect that the $\pi(S_P)$ and $\sigma(S_P)$→ Cu(II) LMCT absorptions for ***rac*-6** will be lower in energy than those from the S_T donor atoms, reflecting greater stabilization of the S_T orbitals by coordination to an additional Cu(I) ion. Further, their intensities should be approximately 50% smaller than those of **24** and ***R,R*-7**, which have two equivalent S_P donor atoms per Cu(II). The separations of the π(S) and σ(S) → Cu(II) LMCT bands in the other four compounds range from 3600 to 5100 cm^{-1}. These spectroscopic benchmarks are consistent with the assignments proposed for the analogous absorptions in ***rac*-6**: specifically, $\pi(S_{P,T})$ and $\sigma(S_{P,T})$ absorptions each separated by about 3000 cm^{-1}, with overlap of the $\sigma(S_P)$ and $\pi(S_T)$ → Cu(II) LMCT bands. This assignment accounts for the relatively intense combined absorption at 23 800 cm^{-1} and the neighboring flanking absorptions at lower and higher energy. The remaining observable bands are assigned as Cu(I) → $S_{P,T}$ MLCT.

Conclusions

Complex ***rac*-2** serves as a useful building block for homovalent and mixed-valence polynuclear thiolate complexes. Structural and spectroscopic trends in the complexes facilitate assignment of their rich UV−vis electronic spectra. This work provides the first approach toward developing a detailed assignment of the individual ligand Rydberg, LF, LMCT, MLCT, and possible MMCT absorptions in such complexes. Metal−ligand bond distances and angles in the mononuclear building blocks **8** and ***rac*-6** are little changed by their incorporation into mixed-valence cluster complexes. LF and π,σ(S) → Cu(II) LMCT absorptions in these monomers are modestly red-shifted in the clusters, as expected from a reduced LF of Cu(I)-coordinated thiolate along with the near structural invariance of the cluster subunits. Structural and spectroscopic studies of ***rac*-6** suggest the presence of a weak Cu(I)−Cu(II) interaction either through space or via a thiolate bridging ligand.

While most bands in the deconvoluted spectra are plausibly assigned, some ambiguities remain. Their removal requires detailed electronic-structural calculations and/or synthesis and spectroscopic analysis of pentanuclear analogues with Cu(II) replaced preferably by Zn(II) to eliminate the LMCT bands or by Ni(II) to blue-shift them.

Acknowledgment. Variable-temperature magnetic susceptibility studies were performed in the laboratory of Professor Martha Greenblatt, and electrochemical studies were performed in the laboratory of Professor Stephan Isied with the assistance of Dr. Riasat Mobashar. We thank Dr. Tom Emge for crystallographic assistance in the modeling of the disordered lattice species in the crystal containing ***R,R*-7**.

Supporting Information Available: Tables in CIF format containing (1) additional details regarding solution of the structures and modeling of the two disorders, (2) information on data collection and refinement of the structures, (3) atomic coordinates, (4) anisotropic thermal parameters, (5) bond lengths, and (6) bond angles for ***rac*-2**, ***rac*-5**·2ClO_4, ***rac*-6**·2DMF, and ***R,R*-7Cl**·solvate. This material is available free of charge via the Internet at http://pubs.acs.org.

IC020156V

(36) Breeze, S. R., Wang S. *Inorg. Chem.* **1996**, *35*, 3404−3408.